폐루프 유압 에너지 회생 시스템에 관한 연구
Design and Assessments of a Closed-loop Hydraulic Energy-Regenerative System

호 치엣 흥 · 윤종일 · 안경관
H. T. Hung, J. I. Yoon and K. K. Ahn

Key Words: Energy Recovery(에너지 회생), Hydraulic Accumulator(유압 축전기), Hydraulic System(유압 시스템), Secondary Control(2차 제어)

Abstract: In this study, a novel hydraulic energy-regenerative system was presented from its proposal through its modeling to its control. The system was based on a closed-loop hydrostatic transmission and used a hydraulic accumulator as the energy storage system in a novel configuration to recover the kinetic energy without any reversion of the fluid flow. The displacement variation in the secondary unit was reduced, which widened the uses of several types of hydraulic pump/motors for the secondary unit. The proposed system was modeled based on its physical attributes. Simulation and experiments were performed to evaluate the validity of the employed mathematical model and the energy recovery potential of the system. The experimental results indicated that the round trip recovery efficiency varied from 22% to 59% for the test bench.

기호 설명

C : viscous friction coefficient (Nm/(rad/s))
J : moment of inertia of the flywheel (kgm^2)
$k_{r1,2}$: gains of the two relief valves (bar/V)
K_{sv} : DC gain of the electro-hydraulic displacement control ($(m^3/rad)/V$)
m_v : mass of vehicle (kg)
p : pressure of the gas in the accumulator (Pa)
q : flow rate into the accumulator (m^3/s)
$Q_{b1,2,3,4}$:boots flow rates
Q_{loss} : volumetric losses of a hydraulic pump/motor (m^3/s)
Q_{ma} : actual flow rate into the inlet port of the motor (m^3/s)
Q_{mi} : flow rate from the motor outlet port (m^3/s)
Q_{pa} : actual flow rate from the pump outlet port (m^3/s)
Q_{pi} : actual flow rate into the inlet port of the pump (m^3/s)
$Q_{r1,2}$: flow rate via relief valve $V_{1,2}$ (m^3/s)
T : temperature of the gas (^0K)
T_a : actual torque of a hydraulic pump/motor (Nm)
T_{ex} : external torque (Nm)
T_{loss} : torque losses of a hydraulic pump/motor (Nm)
V_0 : volume of fluid in the hose between the pump and the motor (m^3)
v : specific gas volume [m^3/kg]
α : absolute value of displacement ratio of pump/motor $PM_{1,2}$
$u_{1,2}$: displacement control input ratios of pump/motors $PM_{1,2}$
$\triangle p$: pressure difference between two ports of a hydraulic machine (Pa)
$\eta_{t(P/M)}$, $\eta_{v(P/M)}$: mechanical and volumetric efficiency of the pump/motor
ω : absolute value of speed of the pump/motor (rad/s)
$\omega_{i,0}$, $\omega_{i,t}$: initial and current (t) speed of pump/motor PM_i (rad/s)

접수일 : 2010년 6월 18일
안경관(책임저자) : 울산대학교 기계자동차공학부
E-mail : kkahn@ulsan.ac.kr, Tel : 019-551-2282
호치엣흥, 윤종일 : 울산대학교 기계자동차공학과

1. Introduction

Energy saving has become an increasingly interesting issue due to increases in fuel price and environmental pollution. Many energy-saving systems have been studied with the aim of reducing energy consumption and exhaust emissions in industrial and mobile applications. In these systems, the majority of the energy-saving benefits were achieved by applying regenerative braking. That is, the kinetic or potential energy of the system was recovered instead of being dissipated by heat transfer. A secondary energy storage system was employed to store the recovered energy. Energy-saving systems were classified based on the type of secondary storage: electric, mechanical, and hydraulic systems use batteries, a flywheel, and a hydraulic accumulator, respectively. Hydraulic energy-saving systems have been considered as a promising solution because of their high recovery efficiency and high specific power [1].

In hydraulic systems, hydrostatic transmissions (HST), constant pressure systems (CPS), secondary control systems with two common rails (CPR), and electro-hydraulic actuators (EHA) have been considered as energy-saving systems. In the above systems, the primary energy was saved because there were not losses via the throttling control as in traditional hydraulic valve systems [2]. In the HST systems, speed of the motor was continuously controlled by adjusting the pump's flow rate. The speed of the load was totally decoupled from the speed of the primary power source, the engine, which improved the efficiency of the engine and the maneuverability. Thus, they were suitable for earth moving machines such as wheel loaders, tractions and forklifts [3]. However, the HST systems cannot recover the kinetic energy of the load, restricting their energy-saving potential. Unlike the HST systems, the CPS systems employ a flywheel with an auxiliary hydraulic pump/motor so that they are able to recover the kinetic energy of the load and reuse the recovered energy. CPS system studies [4-5] have shown that these systems are adequate for mobile applications, such as vehicles. The energy consumption of such vehicles was significantly reduced when compared with those of traditional vehicles. However, the use of the high-speed flywheel has challenges of the dynamic problem of the flywheel when applied to real vehicles. The recovery and reuse of the CPS system were achieved through a cycle that began at the pump, went through the motor, to the flywheel, and then back from the flywheel to the pump, to the motor, and finally to the load. If the efficiency of one component was low, which often occurred for the flywheel pump/motor [4], the overall round-trip efficiency was very low. In EHA systems, batteries or super-capacitors are employed to store the kinetic energy of the load [6]. Although an EHA system has high recovery efficiency and good performance, its low specific power and high price restrict its applicability. Moreover, in practical mobile applications, the primary power source is usually a combustion engine because the addition of electric motors, generators, and batteries in a limited space is not a viable solution.

The CPR system was developed in the early 1980s. Two common rails were employed in the system: a high-pressure line connected with high-pressure accumulators and a low-pressure line connected directly to a tank. The system looked like an electric network. Thus several secondary units could be used both simultaneously and independently. Pumps were used to control the pressure, while the speeds of the loads were controlled by adjusting the displacements of the

secondary units. CPR systems have been shown to have good performance and energy-saving potentials in several applications [7]. However, the secondary unit's low efficiency, influence on other units, and fluid inertia are disadvantages of such systems. The CPR system is applied to vehicles and shows great energy consumption reduction [8-10]. However, they have only been represented through simulation and need to be validated via experiment.

This paper proposed a novel closed-loop HST system with two hydraulic accumulators. The system had energy recovery potential and good performance. The pump and the pump/motor in the proposed system were pressure coupled to improve the efficiency of the primary power source. Because of the novel structure of the proposed system, the efficiency of the secondary unit could be improved by using high efficiency pump/motors working in the positive region, such as bend axis pump/motors. The pump supplied only a load, which could improve the efficiency and performance of the load [11].

2. Proposed system

2.1 Principle of operation

Figure 1 shows the schematic of the proposed system. In comparison with a traditional HST system, the directional control valve and two hydraulic accumulators (HA_1, HA_2) are added. The high-pressure accumulator HA_1 functions as a storage system or a power supply. The low-pressure accumulator HA_2 functions as a low pressure, high-flow source for the hydraulic pump/motor PM_2 during recovery, and the boots system while driving. The flywheel simulated the practical load. The secondary unit and the pump/motor PM_2 could function as a hydraulic pump or a hydraulic motor depending on the speed, displacement and pressure difference between the two ports of PM_2. Figure 2 shows the four-quadrant operation of the secondary unit. If PM_2 worked in quadrants I or III, the flywheel would be powered by the system; however, if PM_2 operated in quadrant II or quadrant IV, the system recovered the kinetic energy of the flywheel.

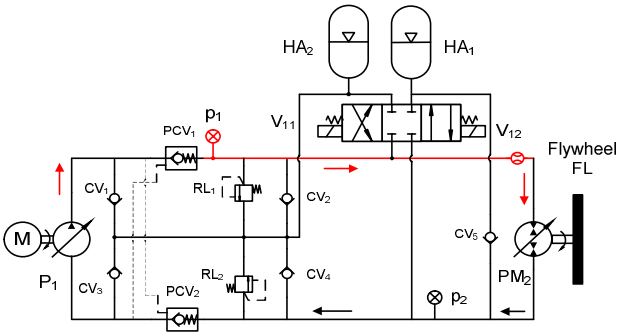

Fig. 1 Proposed system

In the proposed system, driving and braking were distinguished via control of the directional valve. Figure 3 shows the driving phase of the system where p_1 became the high pressure and either the accumulator HA_1 or the electric motor M powered the flywheel. The pilot check valve PCV_2 was opened, and the system was in a semi closed-loop circuit. PM_2 was controlled to activate during quadrant I operation.

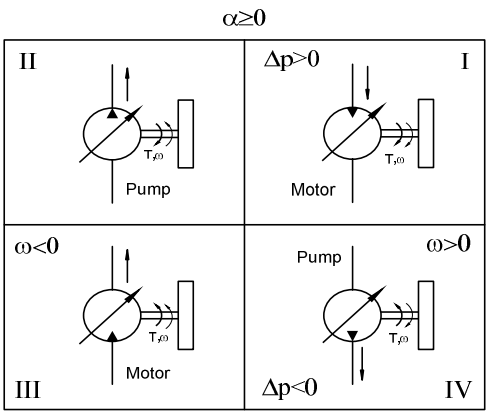

Fig. 2 Four-quadrant operation of the secondary unit

During braking, solenoid V_{12} was engaged and pump P_1 was deactivated. Pressure p_1 was decreased and the pilot check valve PCV_2 was closed. The pressure p_2 increased and PM_2 worked in quadrant IV. Therefore, the kinetic

energy of the flywheel was transformed into hydraulic energy and was stored in the high pressure accumulator HA_1. Furthermore, the use of check valves $CV_{1,2,3,4,5}$ prevented cavitation and absorbed the peak pressure in p_2 when the directional was switched.

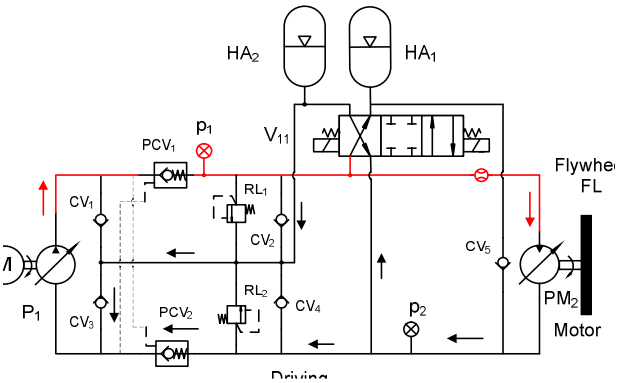

Fig. 3 Driving phase of the system

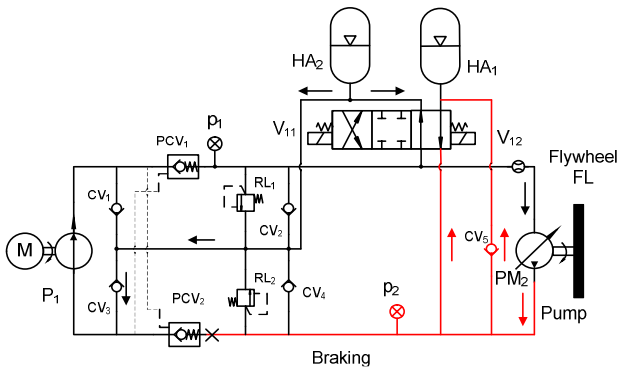

Fig. 4 Braking phase of the system

2.2 System Modeling

In this paper, we ignore dynamic of the clutches and the directional control valve. Main components in the system are modeled as follows.

2.2.1 Hydraulic pump/motor

2.2.1.1 Hydraulic pump

The ideal volumetric flow rate of fluid through a hydraulic pump/motor is expressed by Eq. (1),

$$Q_i = \alpha w D_{\max} \quad (1)$$

In an ideal hydraulic machine without any mechanical loss, the mechanical torque at the machine shaft is expressed in Eq. (2),

$$T_i = \alpha \Delta p D_{\max} \quad (2)$$

In a practical pump, inlet restriction, leakage, and fluid compressibility all reduce the actual flow rate. Pump volumetric efficiency was defined as the ratio of the actual flow rate Q_a to the ideal flow rate Q_i, as expressed by Eq. (3),

$$\eta_{vP} = \frac{Q_a}{Q_i} = 1 - \frac{Q_{loss}}{\alpha w D_{\max}} \quad (3)$$

Viscous torque, Coulomb torque, and hydrodynamic torque losses always exist for a pump, and they must be considered for a practical system. The torque or mechanical efficiency of a hydraulic pump which is a relationship between the actual and the ideal value is estimated by Eq. (4),

$$\eta_{tP} = \frac{T_i}{T_a} = \frac{T_i}{T_i + T_{loss}} = \frac{1}{1 + \frac{T_{loss}}{\alpha D_{\max} \Delta p}} \quad (4)$$

2.2.1.2 Hydraulic motor

The volumetric and mechanical efficiencies are expressed by Eqs. (5) and (6), respectively.

$$\eta_{vM} = \frac{Q_i}{Q_a} = \frac{Q_i}{Q_i + Q_{loss}} = \frac{1}{1 + \frac{Q_{loss}}{\alpha D_{\max} w}} \quad (5)$$

$$\eta_{tM} = \frac{T_a}{T_i} = \frac{T_i - T_{loss}}{T_i} = 1 - \frac{T_{loss}}{\alpha D_{\max} \Delta p} \quad (6)$$

From above equations, T_{loss} and Q_{loss} are the torque and the volumetric losses of a hydraulic axial machine. In this paper, we employ experimental values of T_{loss} and Qloss as shown in [12]. The volumetric losses of an axial hydraulic machine depend on the absolute values of displacement ratio α, the speed ω and the operating pressure $\triangle p$ of the machine and is expressed in Eq. (7).

$$Q_{loss}(\alpha, w, \Delta p) = \Delta q_1 + \Delta q_2 + \Delta q_3 \quad (7)$$

$$\Delta q_1 = 1.76 \times 10^{-7} (w/2\pi) + 1.7 \times 10^{-13} \Delta p \quad (8)$$

$$\Delta q_2 = 5.80 \times 10^{-13} (w/2\pi) D_{\max} \Delta p \quad (9)$$

$$\Delta q_3 = (5.10 \times 10^{-14} - 2.83 \times 10^{-14} \alpha)(w/2\pi) \Delta p \quad (10)$$

where, $\triangle q_{11}$ and $\triangle q_2$ are the volumetric

losses due to leakage of the machine, $\triangle q_3$ is the volumetric loss due to the compressibility of the fluid. The torque losses of an axial hydraulic machine depend on the absolute values of displacement ratio α, the speed ω and the operating pressure $\triangle p$ of the machine and is expressed in Eq. (11).

$$T_{loss}(\alpha, w, \Delta p) = \Delta T_1 + \Delta T_2 + \Delta T_3 \quad (11)$$

$$\Delta T_1 = 4.27 \times 10^{-2}(w/2\pi) \quad (12)$$

$$\Delta T_2 = 5.84 \times 10^{-2}\alpha(w/2\pi) + 8.02 \times 10^{-4}\alpha^2(w/2\pi)^2 \quad (13)$$

$$\Delta T_3 = 2.5 \times 10^{-7}\Delta p - 8.1 \times 10^{-15}\Delta p^2 \quad (14)$$

where, $\triangle T_1$ is torque loss due to viscosity, $\triangle T_2$ is the torque loss due to leakage and $\triangle T_3$ is the torque loss due to compressibility of the fluid.

2.2.1.3 Electro-hydraulic displacement control mechanism

For variable displacement hydraulic pump/motor, the displacement of the machine is usually controlled by an electro-hydraulic mechanism. Input to the mechanism is electric signal and the output is the angle of the swash plate or the displacement of the machine. Although the mathematical model of the mechanism is a fifth-order system in practical applications a reduced-order model is usually used [13]. A first-order system is used in this study as follows,

$$u(t) = \frac{\tau}{K_{sv}}\dot{\alpha} + \frac{1}{K_{sv}}\alpha \quad (14)$$

where u(t) is the electric signal control, τ is the time constant, K_{sv} is the DC gain.

2.2.2 Hydraulic accumulator

In this paper, the Benedict-Webb-Rubin equation is used [14],

$$p = \frac{RT}{v} + \left(B_o RT - A_0 - \frac{C_o}{T^2}\right)\frac{1}{v^2} + \frac{bRT-a}{v^3} + \frac{aalpha}{v^6} + \left[c\left(1+\frac{\gamma}{v^2}\right)e^{\frac{-\gamma}{v^2}}\right]\frac{1}{v^3T^2} \quad (16)$$

where p, T and v are pressure, temperature and specific volume of the gas, respectively. All other values are empirical constants specific for nitrogen gas, and can be found in [15]. By differentiating equation (16) with respect to time and following Otics Time Constant theory we obtain.

$$\frac{dT}{dt} = \frac{T_0 - T}{\tau_a} - \frac{1}{c_v}\left[\frac{RT}{v}\left(1+\frac{b}{v^2}\right) + \frac{1}{v^2}\left(B_0 RT + \frac{2C_0}{T^2}\right) - \frac{2c}{v^3T^2}\left(1+\frac{\gamma}{v^2}\right)^{\frac{-\gamma}{e^{v^2}}}\right]\frac{dv}{dt} \quad (17)$$

The volumetric flow rate is calculated at each time step so the temperate of the gas can be calculated. Thus, the pressure of the gas can be estimated. τ_a thermal time constant of the accumulator it is a experimental parameter. In this study, the gas pressure is assumed to be the fluid pressure in the hydraulic system.

2.2.3 The connecting lines

In this study, losses due to the length of the pipe are ignored. Continuity equations were used to model the pressure of the fluid in the hose. Depending upon the configuration of the system, two distinct systems could be modeled. In braking, pressure in the line L_1 is assumed to be gas pressure of the low pressure accumulator LP. Hydraulic accumulator LP is large, so the pressure in the low pressure line is considered a constant pl. Pressures in the high pressure lines in driving and braking are modeled similarly, so only driving phase is presented here.

2. 2. 3. 1 Flow coupling configuration

Pressure in the high pressure line is similar to the gas pressure in LP, and pressure in the low pressure line is similar to the gas pressure in LP. Gas pressure or fluid pressure in the pressure coupling configuration is determined by the accumulator's parameters and the flow rate into it. Flow rate into the high accumulator is expressed by Eq. (22),

$$Q_a = Q_{pa} - Q_{r1} - Q_{ma} \quad (22)$$

The gas volume can be estimated from the flow rate into the accumulator using Eq. (23),

$$V = V_{0a} + \int_0^t Q_a dt \quad (23)$$

2.2.3 Flywheel

The dynamic equation of the flywheel is obtained by applying Newton's second law, as

in Eq. (24),

$$T_m = J\dot{w} + Cw + T_{ex} \quad (24)$$

T_m is presented in Eq. (6), the pressure difference is defined by Eq. (25), T_{ex} is the braking torque in this study.

$$\Delta p = |p_1 - p_2| \quad (25)$$

In addition, to estimate recovery potential of the system recovered efficiency is defined by Eq. (26). That is the ratio of kinetic difference of the flywheel FL_1 and that of the FL_2 before and after brake.

$$\eta_r = \frac{E_1}{E_2} \times 100 = \frac{\frac{1}{2}J_1(w_{1,t}^2 - w_{1,0}^2)}{\frac{1}{2}J_2(w_{2,0}^2 - w_{2,t}^2)} \times 100 = \frac{w_{1,t}^2 - w_{1,0}^2}{w_{2,0}^2 - w_{2,t}^2} \times 100 \quad (26)$$

Energy restored in the hydraulic accumulator is estimated by Eq. (27),

$$E_a = \int q\Delta p dt \quad (27)$$

3. Test bench system and experimental programs

3.1 Test bench system setup

To validate the ability of the proposed system, a model system was developed for a 2000 kg vehicle. The final reduction gear ratio was 3.55:1, the radius of the wheel was 0.28 m, and the scale model factor of the recoverable energy was 15:1. The parameters of the test bench are shown in Table 1.

Table 1. Parameters of the systems

Main Parameters of the proposed system	Value	Unit
Maximum displacements of $PM_{1,2}$	55	cm^3/rev
Moment of inertia of the flywheel	2.5	$kg.m^2$
Viscous friction coefficient	0.01	Nm.s /rad
Hydraulic accumulators volumes	20, 60	Liters
Pre-charge pressures in the accumulators	120, 2	bar

The schematic and photograph of the test bench are shown in Figs. 5a and 5b, respectively. For the test bench, the hydraulic pump/motors HPV55-02 were employed. The hydraulic accumulators were Hyundai Oil Products, and the directional control valve was from the Atos RPE4 series with a max flow rate of 120 LPM. The pressure and flow sensors were employed from Websters Instruments LPT and LTE series, respectively, and the tachometer and torque transducer were SETech products.

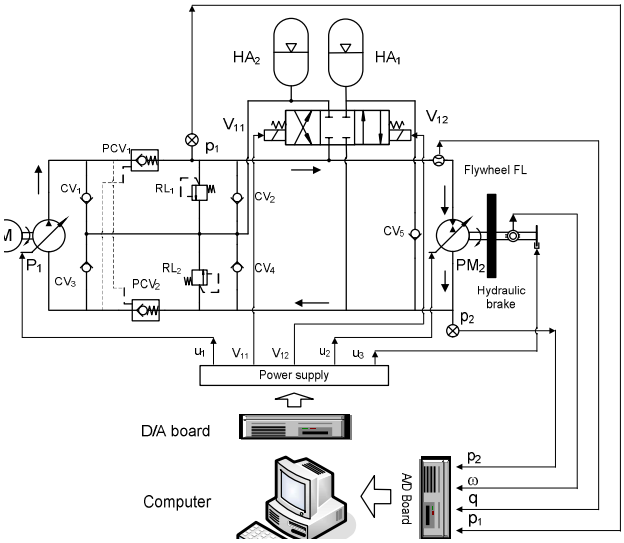

Fig. 5a. Schematic diagram of the test bench system

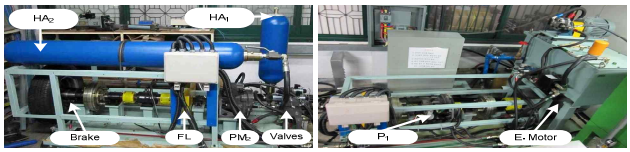

Fig. 5b. Photograph of the test bench

The control and data acquisition systems were controlled by a personal computer and 12 bit A/D and D/A boards 1720 and 1711 of Advantech products. The control system was designed in Matlab Simulink, where the sampling time was 2 ms.

3.2 Experimental programs

3.2.1 Flywheel test and estimation of the round-trip efficiency

A cycle of energy recovery was defined as follows. The kinetic energy of the flywheel was transferred to the accumulator as potential energy in the form of a high-pressure fluid, which then transformed

the stored energy back into kinetic energy via the flywheel. From the viewpoint of the component's efficiencies, the round-trip efficiency was defined by Eq. (28),

$$\eta_{rt} = \eta_{fl,d}\eta_p\eta_{ac}\eta_m\eta_{fl,a} \quad (28)$$

where η_{fl}, $\eta_{m/p}$, and η_{ac} are the efficiencies of the flywheel, PM_2, and the accumulator, respectively. The efficiencies of the flywheel during deceleration ($\eta_{fl,d}$) or acceleration ($\eta_{fl,a}$) depended on the particular application. For the estimation of the round-trip efficiency of the system, the efficiency of the accumulator was assumed to be a constant, 0.95. The motor efficiency was in the interval [0.6 0.94] and the pump efficiency was in the interval [0.68 0.92].

The key to energy recovery was the flywheel, so its characteristics should be taken into account when analyzing the regenerative cycling data. The kinetic energy of the flywheel was lost gradually due to the friction of the particular simulated system. The test was conducted as follows. The flywheel was driven to 1100 rpm, at which time pump P_1 shut off and the displacement of PM_2 was controlled to zero. A few identical tests were conducted to test the repeatability. The results of the simulation and the experiment are shown in Fig. 6, which showed agreement. Under the test conditions, the energy of the flywheel was significantly reduced for operations longer than 10s. However, the braking time in most applications was only a few seconds, so the system could still be considered suitable as a regenerative energy simulator system.

The efficiencies of the flywheel were assumed to be constant and similar during both deceleration and acceleration. The determination of the efficiency based on Fig.6 is as follows. Assuming a deceleration time of 3 s, the energy of the flywheel decreases from $E_0 = \frac{1}{2}J\omega_0^2$ to $E_3 = \frac{1}{2}J\omega_3^2$, so the efficiency η_{fl} is estimated using Eq. (27) to be $\eta_{fl} = \frac{E_3}{E_0} = 0.9$. As seen in Fig. 6, η_{fl} varied from 0.9 to 0.52 with respect to a deceleration time increase from 3 s to 10 s. Therefore, using Eq. (28), the round-trip efficiency of the test bench varied from 32% to 66% when the braking time was less than 10 s.

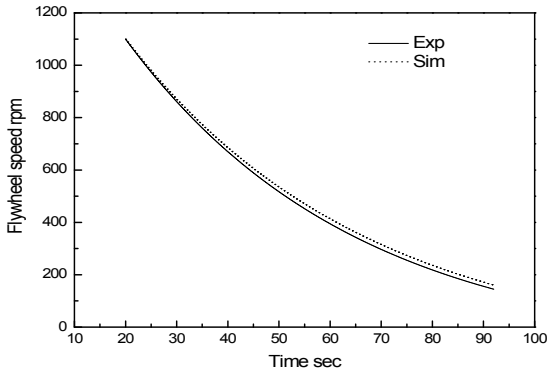

Fig. 6 Flywheel test

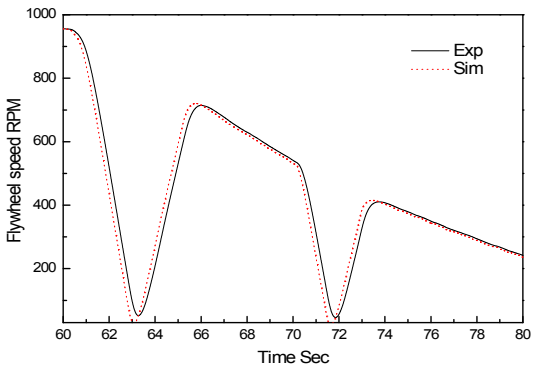

Fig. 7 Speed of the flywheel(u_2=0.75)

3.2.2 Basic tests

This test was used to evaluate the validity of the employed mathematical model. The experimental round-trip efficiency was defined by Eq. (26). The speed of the flywheel in the equation was a measured value. The test was conducted at four initial flywheel speeds, corresponding to four displacement ratios. For each test, when the speed of the flywheel reached the setting value, pump P_1 was shut off and valve V_{12} was turned on. When the speed of the flywheel was nearly zero, V_{12} was shut off and V_{11} was turned on and the

speed of the flywheel increased again. Figure 7 shows the speed curve of the flywheel in two cycles of energy-recovery. The figure also shows that the simulation model validated the test.

Figure 8 shows the simulation and experimental results for the pressure of accumulator HA_1. As seen in the figure, the pressure in the accumulator increased from the 60th second to the 63rd second and decreased again until the 65th second. The next recovery cycle was taken occurred in the interval from the 70th to the 73rd seconds. Obviously, the initial kinetic energy of the flywheel was small and the cycle of the recovery was short. The measured pressure was slightly lower than the simulation pressure, so the measured round-trip efficiency of the test bench would be lower than the estimated value in the previous subsection.

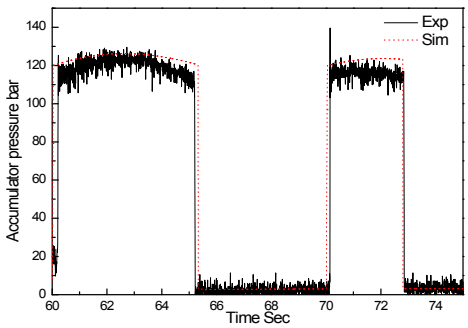

Fig. 8 Pressure in the high pressure line

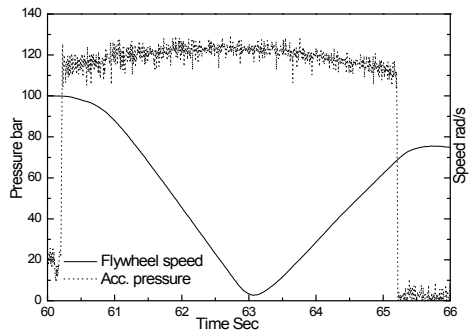

Fig. 9 Measured speed and pressure

Figures 9 and 10 show more detail about energy transformation in the system. The pressure in the accumulator increased from 120 bar to 130 bar, corresponding to a flywheel speed that decreased from 100 rad/s to nearly 0 rad/s at the 63rd second. Then, the speed of the flywheel increased again, but the pressure decreased from 130 bar down to 120 bar at the 65th second. The flywheel's maximum speed was 73 rad/s and the round-trip efficiency was 53%. Figure 10 indicates that the accumulator recovered 8.3 kJ of the flywheel's 12.5 kJ of kinetic energy and again generated 6.7 kJ of the flywheel's kinetic energy in the next cycle. Thus, the recovery efficiency in this case was 66.4%, while the reuse efficiency was 80.7%.

Figure 11 shows values of p_2 when valve V_{12} was switched from off to on. The pressure increased slightly at the beginning due to the delay of the directional control valve. In the system, the use of the check valve CV_5 prevented a high-pressure peak. As a result, the pressure did not increase much and thus was acceptable for practical applications.

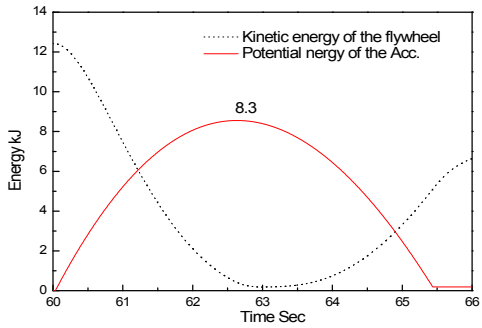

Fig. 10 Measured energy of the system

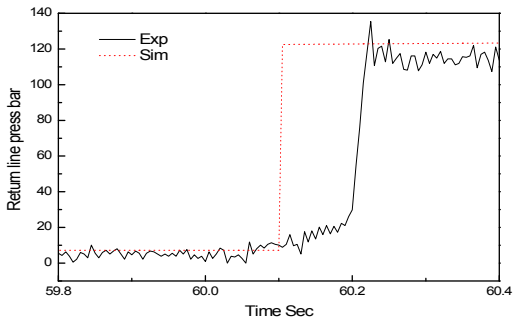

Fig. 11 Pressure p_2 when V_{12} : OFF -> ON

Figure 12 shows the measured round-trip efficiency of the system versus the initial speed and displacement ratio of PM_2. In these tests, accumulator HA_2 was pre-charged to 10

bar. From the figure, the maximum and minimum round-trip efficiencies were 59% and 22%, respectively. The results were lower than the estimated results in the previous section because the braking time of the system in the case of α= 0.5 was greater than 10 s. The round-trip efficiency significantly decreased with the low displacement ratio.

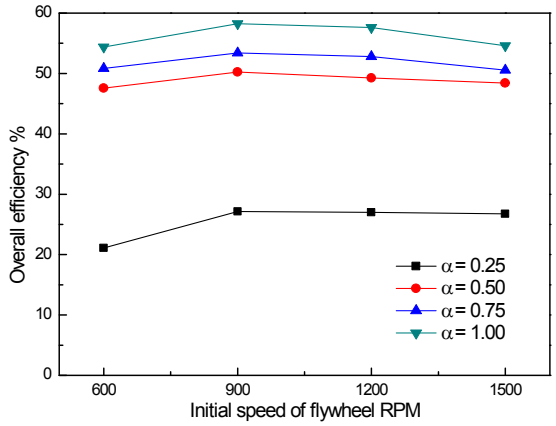

Fig. 12 Measured round-tip efficiency

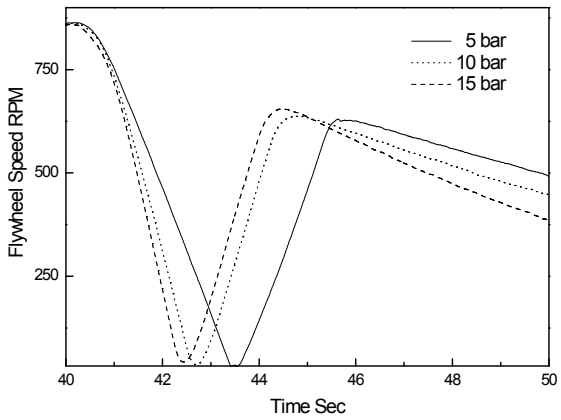

Fig. 13 Speed versus the suction port pressure

Figure 13 shows that the pre-charge pressure of HA_2 impacted the round-trip efficiency of the system. The figure implies that if the pre-charge pressure was not suitable, the recover efficiency would be low.

4. Conclusion

A novel hydraulic energy-saving method was developed from modeling through simulation and finally to experimental validation. The experimental results confirmed the validity of the employed mathematical model and the energy-recovery potential of the system.

The study indicated that the round-trip efficiency of the system varied from 22% to 59% depending on the operating pressure, displacement, and speed of the secondary unit.

후 기

본 연구는 2단계 BK21 사업의 지원을 받아 이루어졌습니다.

참고 문헌

1) L. Guzzella, A. Sciarretta, Vehicle Propulsion Systems : Introduction to Modeling and Optimization, Springer, 2007.
2) M. Jelali, A. Kroll, Hydraulic Servo-system, second ed., Springer, 2004.
3) K.E. Byberg, Hydrostatic Drives in Heavy Mobile Machinery - New concept and Development trends, Society of Automotive Engineer, 1997.
4) H. Shimoyama, S. Ikeo, E. Koyabu, K. Ichiryu, S. Lee, Study on Hybrid Vehicle Using Constant Pressure Hydraulic System with Flywheel for Energy Storage, SAE 2004-01-3064.
5) K.K. Ahn, T.H. Ho, Q.T. Dinh, A study on energy saving potential of hydraulic control system using switching type closed loop constant pressure system, Proc. of the 7th JFPS, Toyama, (2008) 317-322.
6) H. Yang, W. Sun, B. Xu, New investigation in energy regeneration of hydraulic elevators, IEEE/ASME transaction on mechatronic 12 (2007) 519-526.
7) R. Kordak, Hydrostatic transmission drives with secondary control, Bosh Rexroth AG, 2003.
8) R. Johri, Z. Filipi, Low-cost pathway to ultra efficiency car: Series hydraulic hybrid system with optimized supervisory control,

SAE, 2009-24-0065.
9) P. Matheson, J. Stecki, Modeling and simulation of a fuzzy logic controller for a hydraulic hybrid powertrain for use in heavy commercial vehicles, SAE, 2003-01-3275.
10) Y.J. Kim, Z. Filipi, Simulation study of a series hydraulic hybrid propulsion system for a light truck, SAE, 2007-01-4151.
11) R. Rahmfeld, Development and control of energy saving hydraulic servo drives, Proc. of 1st FPNI-PhD symposium, Hamburg, (2000) 167-180.
12) Hao, J., Ikeo, S., Sakurai, Y., and Takahashi, T. Energy Saving of a Hybrid Vehicle Using a Constant Pressure System, *JFPS*, 1999, 30(1), 20 - 27.
13) Kim, C. S. and Lee, C. O., Speed control of an overcenetered variable displacement hydraulic motor with a load torque observer, *Control Engineer Practice,* 1996,4, 1563-1570.
14) Matheson, P. and Stecki, J. Development and Simulation of a Hydraulic-Hybrid Powertrain for use in Commercial Heavy Vehicles, *SAE*, 2003, 2003-01-3370.
15) Sonntag, R. E., Borgnakke, C. and Van Wylen, G. J. Fundamentals of Thermodynamics, 5th Edition, *John Wiley and Sons*, New York, 1998.